PARALLEL COMPUTATION OF ORBIT DETERMINATION FOR SPACE DEBRIS POPULATION

Estrella Olmedo [(1)], Noelia Sánchez-Ortiz[(2)], Mercedes Ramos-Lerate[(3)]

[(1)]DEIMOS Space S.L. Ronda de Poniente 19, 2º2, Tres Cantos, Madrid, 28760 Spain, Email: estrella.olmedo@deimos-space.com

[(2)]DEIMOS Space S.L. Ronda de Poniente 19, 2º2, Tres Cantos, Madrid, 28760 Spain, Email: noelia.sanchez@deimos-space.com

[(3)]DEIMOS Space S.L. Ronda de Poniente 19, 2º2, Tres Cantos, Madrid, 28760 Spain, Email: Mercedes.ramos@deimos-space.com

ABSTRACT

In this work we present an algorithm for computing Orbit Determination for Space Debris population. The method presents a high degree of parallelism. That means that the number of available computers divides the computational effort.

The context of this work and the later scope is to have the capability of cataloguing and correlating the Space Debris population. In this sense, as better the accuracy provided by the orbit determination is, more accurate will be the estimation of the state vectors corresponding to the debris objects and better will be the accuracy of the future catalogue of Space Debris. As more objects we can determinate the corresponding orbit, more complete will be the future catalogue. Therefore numerical tools for orbit determination are a key point in the development of a future ESSAS.

The first time that a new object is observed, six measurements (these measurements may come from RADAR, Ground Based Telescope or Space Based Telescope) are required for computing an Initial Orbit Determination (IOD). After that, the Initial Estimated State Vector (IESV) is improved within the next-coming measurement.

The idea of this method is the following. From six initial measurements, we compute the IOD following the same ideas of [1]. We compute also the initial knowledge covariance matrix (IKCM) corresponding to the IESV. In general, the numerical error of the IOD is too big for processing the following measurements with a conventional numerical filter (like the Square Root Information Filter (SRIF)). The problem is that the improvement of the accuracy in the IOD is not an easy task in those cases with large initial error. However the computed IKCM give a realistic approximation of the committed error in the IOD. The proposed algorithm uses the IKCM for generating a cloud of IESVs. All the IESV inside the cloud are processed with a new and much smaller IKCM by using SRIF. In such a way that the ones that are close enough to the real state vector (and thus its real IKCM is in agreement with that imposed) survive. Those ones that are far away of the real solution make SRIF to diverge and are skipped from the initial cloud.

We will show numerical results and we will compare the accuracy with the numerical results obtained by applying directly the results of the IOD to the SRIF. Implementation of the algorithm in a cluster of PCs will also be addressed.

The reported algorithm has been implemented in the Advanced Space Surveillance System simulator (AS4) and developed by DEIMOS Space. The project has been partially funded by the CDTI (Ministerio de Ciencia e Innovación (Spanish Government)).

1. INTRODUCTION

In this work we have developed and implemented an algorithm for computing orbit determination for space debris population. The algorithm presents high degree of parallelism. The work has been structured as follows. In this section we will describe the debris population as well as the dynamical models of motion used in our numerical simulations. We will also describe the technical characteristics of the simulated radar and optical sensors. After that, section 2 speaks about the IOD computation and the IKCM computation. Some numerical results are provided in terms of achieved IOD accuracy. In section 3 we explain how the orbit determination is classically computed and which are its numerical limitations. Section 4 explains which is the idea of the new algorithm for orbit determination computation and how it can be implemented in a cluster of PCs. It also includes a subsection with the numerical results. This work finishes with a section of conclusions.

Proc. '5th European Conference on Space Debris', Darmstadt, Germany 30 March – 2 April 2009, (ESA SP-672, July 2009)

1.1. Space Debris Population

The population that will be considered for the numerical simulations has been provided by ESA (European Space Agency). W consider the following classification of the Space Debris population type of orbits:

- **Low-Earth Orbits (LEO):** They are the orbits that are located closest to the earth. All these orbits which apogee is lower than 2000 km are considered LEO type orbits. There are 194,612 LEO type orbits in our considered population (11,110 of them are greater than 10 cm).
- **Medium-Earth Orbits (MEO):** We consider MEO type orbits; the ones with inclination lower than 67º and mean motion greater than 1.5 but smaller than 2.5 revolutions per day. In our database there are 33,447 MEO type of orbits (972 of them are greater than 10 cm).
- **Geosynchronous Orbits (GEO):** All these orbits with perigee greater than 34,000km and apogee smaller than 38,000km are considered GEO type orbits. There are 81,711 GEO type of orbits in our database (3,322 of them greater than 10cm).
- **GEO transfer Orbits (GTO):** All these orbits with perigee smaller than 20,00km and apogee between 30,000 and 45,000km are considered GTO type of orbits. There are 13,426 GTO types of orbits in our database, 92 of them are greater than 10cm.
- Finally, all orbits that are not any of the previous type of orbits are considered Other (OTH) type of orbits.

Fig.1 shows the distribution of diameter vs Semi-major axis and eccentricity vs. semi-major axis.

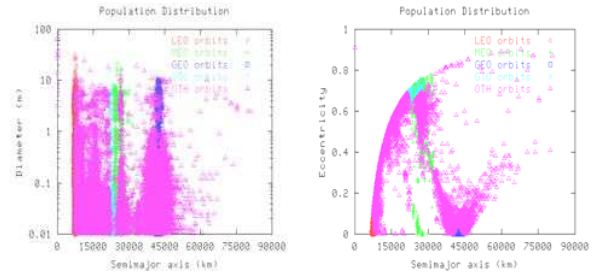

Fig.1: Distribution of Debris. The pictures correspond to the graphics of semi-major axis vs diameter (on the left) and semi-major axis vs Eccentricity

1.2. The dynamical Model of Motion

In order to simulate the generation of measurements we need a model of the real motion of these space objects. On the other hand, the observer, who receives the measurements, needs an estimated model of motion. This model has not the complete dynamical information but it must be close to the real model. Therefore, two different models of motion are considered in order to simulate the procedure of orbital determination.

On one hand, the real model of motion: it will be used for simulating the real dynamics; in concrete using this model of motion generates the measurements. In this case, the gravitational field is the sum of the following forces.

- **Kepler:** the main contribution, to consider the force of the Earth over the debris object.
- **Earth gravitation potential:** the software allows a development of the series up to 50th order (GEMT3). However in our simulations we will use only a 4 tesseral x 4 zonals series.
- **Third bodies:** Sun and Moon contributions are the ones considered in our computation. The position of both bodies is simulated by means of analytical ephemeris.
- **Atmospheric contributions.** We use the Jacchia-Linaberry model in our simulations.
- **Simple Solar Radiation Pressure model**

The three first forces are conservative and they do not depend on the area to mass ratio, while the two last contributions are dissipative and they depend on the area to mass ratio. Moreover as the real effect of the atmosphere and solar radiation pressure are not well known over the debris objects, the last two contributions include a Gauss Markov noise. Gauss-Markov noise refers to a correlated stochastic noise with a given autocorrelation time τ and a given covariance σ_g.

The following dynamic noise is assumed in our simulations:

- Atmospheric Drag error modelled as a Gauss-Markov noise with a 1-sigma value of 15% and autocorrelation time of 100 minutes (see Fig.2).
- Solar radiation Pressure error modelled as a Gauss-Markov noise with a 1-sigma value of 15% and autocorrelation time of 100 minutes (see Fig.2).

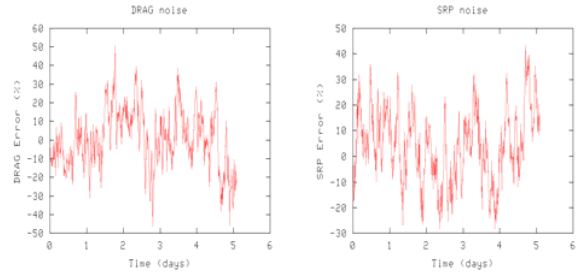

Fig.2: Atmospheric drag error behavior (on the left) and solar radiation pressure error behavior (on the right).

In the estimated model of motion, the noise corresponding to DRAG error and the noise corresponding to SRP error are not known. The other contributions are the same as in the real world, but these noises must be estimated. Moreover, in order to apply DRAG and SRP forces, the mass and the diameter of the object must be also known or estimated.

Of course, not all forces affect with the same intensity to each object in the Debris population. The intensity of

the forces will depend (mainly) on the location of the object. Fig.3 shows the different contributions for each type of orbits. The plots have been done in the following manner. We consider the initial position of every object of the initial catalogue. At this time, we compute the acceleration corresponding to each one of the acting forces. We plot the acceleration corresponding to Kepler (in red), to the Geopotential (blue), to Sun (green), Moon (dark blue), SRP (pink) and DRAG (yellow).

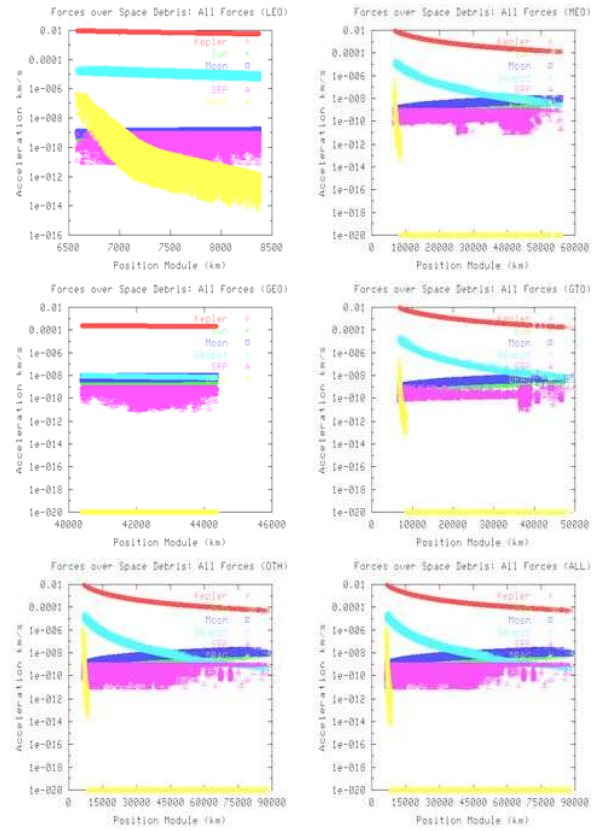

Fig.3: Force Contributions in the Debris population.

As expected, the larger force in all cases is the Kepler contribution. Among the perturbations over Kepler acceleration, importance of the other contribution mainly depends on the type (or concretely, on the position) of the orbit. For those orbits located closer than 45,000km to the Earth, the biggest contribution after Kepler is the corresponding to the Earth gravitational potential, while the orbits that are located farther than 45,0000km from the Earth centre the second most important contribution is the gravitational effect of the Moon. In any case, the second most influent force corresponds to a conservative force. On the other hand the DRAG effect is very high for LEO orbits, or in general for those orbits located closest to the Earth (closest than 7000km to the Earth the effect of DRAG is almost of the order of 10^{-6}).

1.3. Measurement generation

Two different types of measurements are considered in this work

- **Radar measurements,** using a bistatic radar (GRAVES type), which would provide the following observable: Azimuth, Elevation & Doppler.
- **Optical measurements** using 0.5m-diameter telescopes, which would provide the following observable: Azimuth, Elevation. Four different locations have been considered: Marquises Islands, Tenerife, Cyprus and Perth. The pointing of the telescope has been considered as in [1] (see also [2] and [3]). The idea of this strategy is that the telescope is moving in a declination strip (of –17º, 17º) at the rate of one field each 15 seconds (making survey). When it finds a new object, the system predicts when new images are needed in order to get an accurate orbit determination enough for correlation purposes (generally one and two hours after the detection of a new object). At these predicted times, the telescope gives up its survey tasks, goes to catch the required images (follow up images –FUP-) and returns to continue its survey tasks. As a consequence of that, the observation time is shared between survey and tracking, and thus, the capability of finding new objects is reduced.

The simulator used for generating the measurements is the AS4 simulator (see [4] for the first version of the simulator and [2] for later versions). The computation of the observables is performed from the real position and velocity of the debris object. Once the observable has been computed, a Gaussian random noise is added to it.

2. INITIAL ORBIT DETERMINATION COMPUTATION

The problem of Initial Orbit Determination (IOD) consists in computing the position and velocity of an object from its first observation. The mathematical problem has six unknown (three position coordinates and three velocity coordinates). Therefore, at least six measurements are required to compute a first estimation of the state vector of the object. In this sense, it does not matter the sensor where the measurements come from: We can consider three pairs of azimuth and elevation coming from Ground Based Telescope observations; or we can consider the Doppler, azimuth and elevation at two different times of one track observed by one Ground Based Radar; even we could consider six measurements coming from different type of sensors.

In practical purpose, the type of sensor where the measurements come from does (strongly) affect the IOD problem. For instance, it is not the same one ground based telescope that moves the pointing each 15 seconds than one radar that receives signal in a “continuous”

way (it produces tracks of measurements along the visibility period of the object).

2.1. IOD accuracy

In this section, for optical measurements, we will assume that two FUPs are available one and two hours after the detection of the object. We have used the algorithms explained in [1]. The availability of the assumed FUPs is also justified in [1]. Table 1 shows the IOD numerical results obtained for optical measurements.

Table 1: IOD numerical results for optical measurements.

TYPE OF ORBIT	Number of observed objects	Mean Position Error (km)	Mean Velocity Error (m/s)
MEO	154	5.26	0.649
GEO	1061	37.71	2.99
GTO	13	4.19	0.696
OTH	341	43.66	3.238

We compute the IESV in case of radar, from the first and the last measurements (Doppler, azimuth and elevation) of the first observed track. Table 2 shows the IOD numerical results obtained for radar measurements.

Table 2: IOD numerical results for radar measurements.

TYPE OF ORBIT	Number of observed objects	Mean Position Error (km)	Mean Velocity Error (m/s)
LEO	1719	12.02	37.28
MEO	31	10.33	40.51
OTH	158	9.10	36.58

2.2. Initial knowledge covariance matrix (IKCM)

A key point in to efficiently performing the orbit determination process is the calculation of the initial estimated state vector covariance matrix. The object batch orbit determination and correlation by means of a Square Root Information Filter (SRIF) requires a realistic covariance matrix to work optimally (see section 3). The computation of the covariance matrix has been implemented for radar and for telescope IOD computations. The idea is the same in all cases. The IOD is computed from 6 initial measurements. The numerical Jacobian J corresponding to the numerical derivatives of the IESV with respect the six initial angles are computed. The IKCM is computed as:

$$IKCM = J^T \cdot E \cdot J$$

with E a diagonal 6x 6 matrix containing the sigma error of the measurements in its diagonal (see [2] for all details).

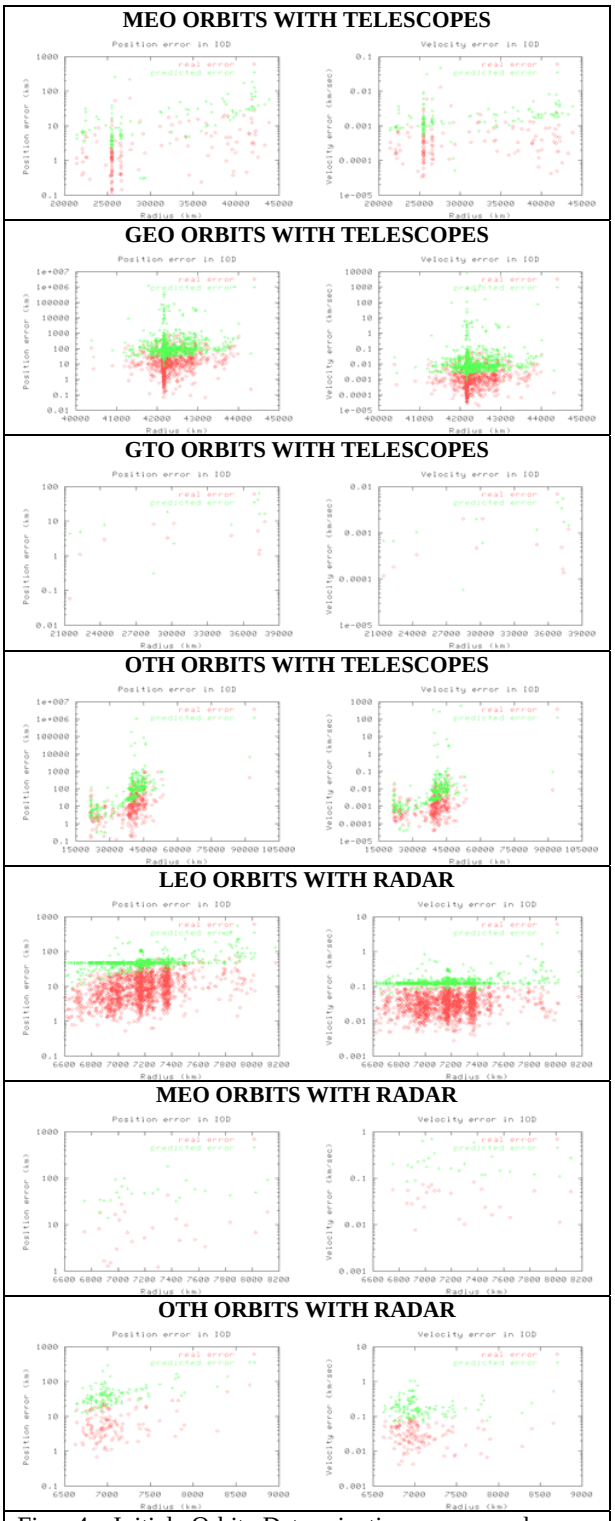

Fig. 4: Initial Orbit Determination error and error predicted by the Covariance Matrix is also shown in the pictures.

In Fig. 4 the numerical IOD error and the predicted IOD error by the IKCM are shown. The green points correspond to three times the sum of the root square each one of the three corresponding components of the Covariance Matrix diagonal (the three position coordinates for comparing the IOD position error and the three velocity coordinates for comparing with the IOD velocity error). That is similar to compare with the 3-sigma of the predicted error. The red points correspond to the real position error (in modulus) or the real velocity error (in modulus). That is the difference between the real state vector and the estimated state vector. In order to have a good behavior of SRIF the IKCM must provide a predicted error greater or equal to the real error. We can observe that the green points are over the red points. Therefore, in our computations the IKCM is quite realistic (some time pessimistic, which is always safer than an optimistic behavior).

3. ROUTINE ORBIT DETERMINATION

The mathematical approach of the routine orbit determination (ROD) problem is the following. At the beginning, IESV and the corresponding IKCM are required. Moreover initial estimation for DRAG and SRP errors are required (see section 1.2). In our computations we always start with an initial estimation of null noise. On the other hand, the effects of the atmosphere and the solar radiation pressure depend on the mass, the diameter, the orientation and the shape of the object. We will consider that we know the relation area to mass. We want to remark that the sensors do not provide the area to mass ratio, and that a priori this parameter is not known.

With all these initial data, the next-coming measurements are processed with a numerical filter. We use a Square Root Information Filter (SRIF) (see [5] for a detailed explanation of the method). In each step, the new measurements are processed with the previous estimation of the state vector, covariance matrix and dissipative noise coefficients (DRAG and SRP). With these data, SRIF computes a new estimation of the state vector with the corresponding covariance matrix and new approximations to the corresponding coefficients of DRAG and SRP noise. And so on with the following measurements.

3.1. ROD accuracy

Table 3 shows the number of objects that the SRIF has not converged for optical measurements when it processed some of its measurements (third column). The last column shows the percentage of objects within bad convergence of SRIF. The percentage of bad convergence of SRIF arrives up to more than the 50 % (for optical measurements and GEO objects) and almost the 90 % (for radar measurements and LEO objects). Radar results are much worse than the corresponding to Telescopes. That may be for two different reasons. On one hand in these cases the initial set of measurements are closer than in Telescope case. They come from the first processed track: the first and the last measurements of the first track. These tracks have duration of few minutes. As closer in time the measurements are, worse is the IOD accuracy, and more difficult is the convergence of SRIF. The second reason is that for those objects, the DRAG effect is very high (see Fig.3). This effect must be estimated and this estimation not always is close enough to the real DRAG value.

Table 3: SRIF divergences for optical measurements

	TYPE OF ORBIT	Total Number of Objects	Objects Bad Conver-gence	Percentage Bad Conver-gence
TELES-COPE	MEO	154	37	24
	GEO	1061	556	52
	GTO	13	2	15
	OTH	341	131	38
RA-DAR	LEO	1719	1538	89.47
	MEO	31	21	67.74
	OTH	158	130	82.27

Table 4: Simulation with all type of orbits. The total number of simulated objects is 1568 for telescopes and 1909 for radar.

	Sigma of IOD position error (km)	Sigma of IOD velocity error (m/s)	Number of divergences	Percen-tage of divergen-ces
Teles-copes	0.1	0.005	0	0
	1	0.05	19	1.21
	10	0.5	442	28.19
	50	5	737	47.00
RADAR	50	5	1578	82.66
	10	0.5	1537	80.51
	1	0.05	984	51.55
	0.25	0.15	335	17.55
	0.1	0.005	94	4.92
	0.025	0.015	22	1.15
	0.001	0.005	15	0.78

A sufficient condition (but not necessary) for obtaining good behavior of the filter is to have the IESV very close to the real state vector (closer than the estimations reported in Table 1) and the IKCM according with this initial error. We mean that if we have an IESV that is almost the real one, with the corresponding IKCM, the filter does not diverge. The problem is that the numerical error required for this, is much smaller that the numerical error acquired with the IOD algorithms. We have considered the full population greater than 10cm and we have generated 5 simulated days of measurements. Then we have performed orbit

determination starting with a pre-configured IOD error. That is we have started with the real state vector with a noise generated by means of a Gauss probability function with a configurable sigma. The IKCM has been considered diagonal with the value of the configured sigma in the diagonal. *Table 4* shows the number of divergences of SRIF of those simulations. When the initial estimated state vector is very close to the real state vector (see the results of the first row) there are not any divergences in the filter. The problem is how can we obtain this accuracy in the IOD?

4. PARALLEL ALGORITHM FOR COMPUTING ORBIT DETERMINATION

In section 3 we have concluded that when the IOD numerical error is very small the filter works without divergences. The problem is that reducing the IOD error is not an easy task. In this section we want to explain a methodology for determining orbits that uses the same IOD algorithm and the same filter (the SRIF) as the ones used in previous sections, but it avoids the divergences of the filter. The proposed algorithm uses the IKCM for generating a cloud of IESV. All the IESV inside the cloud are processed with a new and much smaller KCM by using SRIF. In such a way that the ones that are close enough to the real state vector (and thus its real KCM is in agreement with that imposed) survive to the process. Those ones that are far away of the real solution make SRIF to diverge and are skipped from the initial cloud.

4.1. Algorithm description

The idea of the algorithm is very simple. The SRIF works without problems when the IOD error is small. The accuracy of the IOD algorithms is not small enough but the predicted error by the IKCM is realistic or in the worst cases pessimistic. That means that in a neighborhood (defined by the IKCM) of the initial estimated state vector, we would find the real state vector. Therefore, if we consider a cloud of points randomly distributed in this neighborhood, some of these points would have much small numerical error than the initial considered estimation. The number of points needed to be close enough to the real state vector depends on the realistic or pessimistic that the IKCM is and on the numerical error of the IOD computation.

Fig. 5 illustrates the main idea of this algorithm. The IOD algorithms provide an IESV (the green point) in addition of a IKCM (the green circle) that predicts the error of the estimated vector. We want to have lower error in the initial estimation, so we consider a cloud of points (represented in the picture with yellow and gray points) within a lower imposed Covariance Matrix (Cov) (represented in the picture with a yellow circle). The cloud of points is taken following the IKCM (inside the green circle). But not all these points are close enough to the real state vector. Only the yellow points in the picture are actually according with the predicted error of the imposed Cov (inside the yellow circle). When a new measurement is processed, we increase the knowledge of the estimation. That means that the estimation of the state vector improves and therefore the predicted error by the Cov decrease (in the picture, the circles become smaller when measurements are processed). If we have considered the first imposed Cov small enough (the yellow circle small enough), all the initial estimations according with the corresponding predicted error would not have any problem with SRIF. All yellow points will remain inside the next orange circles. The problem is that we do not know (a priori) which is the best Cov for processing all the measurements. Consequently, some of the points that are initially according with the Cov may diverge when processing the incoming measurements. However, after processing few measurements, the method stabilizes (in the picture after the third measurement the points always remain inside the next-coming circles).

.

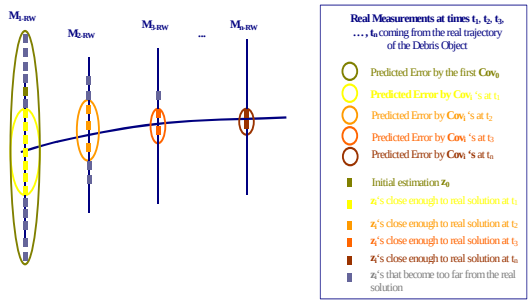

Fig. 5: Illustration of the idea of the OD by means cloud of points.

Let us explain the algorithm with more detail. Let us consider the IKCM, let us say Cov^0, computed as explained in section 2.2 and z^0 the IESV computed like in sections 2.1. Since the IKCM is a positive definite matrix, we can compute the corresponding Cholesky decomposition:

$$Cov^0 = U^T \cdot U$$

with U the upper triangular square root Cholesky factor. We generate a new IESV z^i (with $i=1,\ldots, N$, and N the total number of initial points inside the cloud), following the next equation:

$$z^i = z^0 + U\zeta^i$$

with ζ^i a random vector following a normal function of 0 mean and 1 standard deviation.

In order to apply the SRIF to each one of these initial estimations z^i, we need a Knowledge Covariance Matrix associated to them, let us say Cov^i. We construct Cov^i as a diagonal matrix with: the sigma of the configured ECRVs (corresponding to DRAG, SRP and also the ECRVs corresponding to the added noise in the position

of the Space Based Telescopes) in the first diagonal coordinates; a configurable sigma σ_p in the three position diagonal coordinates; and a configurable sigma σ_v in the three velocity diagonal coordinates. These σ_p and σ_v will indicate to SRIF how is the numerical error associated to z^i. In other words, these σ_p and σ_v will be small for successful orbit determination.

Once, we have generated a cloud of initial estimated state vectors, within their corresponding Covariance matrix, we process the incoming measurements with SRIF (see section 3) for all the points inside the cloud. All these points that, after processing the measurements, whose residuals between estimated measurements and real measurement are greater than $3\sigma_m$ (the sigma of the expected noise in measurements), are skipped from the initial cloud. The points that survive are processed within the following measurements and so on.

4.2. Parallel implementation

The main problem of the algorithm explained in section 4.1 is that the computational time increases. At the beginning, when the first measurements are processed, the number of orbits for computing their OD is multiplied by the number of points considered inside the cloud. This problem disappears when several measurements are processed. After processing several measurements all the points inside the covariance matrix remain there for the rest of in-coming measurements. But at the beginning the method is much more slow than the ones explained in section 3. The good news is that the extra effort required by this algorithm is easily parallelisable. In other words, we can use several available computers to reduce the computational time. *Fig. 6* illustrates how the algorithm can be parallelised.

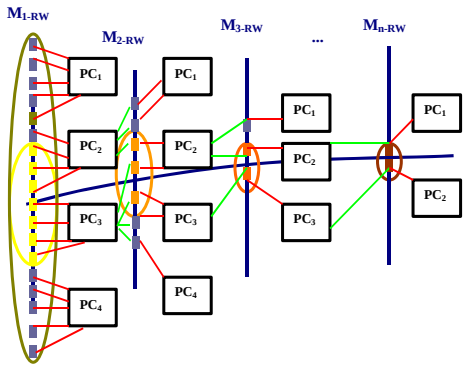

Fig. 6: Illustration of the parallelisation of the OD algorithm within clouds of points

The key point in the implementation is that the task of processing a measurement for one point in the cloud is completely independent on the task of processing the same measurements for another point in the cloud. That means that we can distribute all the points in the cloud into the available computers. Each computer will process its corresponding sub-cloud and will return all these points that have survived. In the next measurement we will have a new cloud. We distribute the points inside the new cloud into the available computers and they carry on computing the orbit determination of each one of the points and they will return the new points that have survived. And so on. At some time, it may happen that we have more computers than points. In this case we will use only the necessary computers. The other computer may be used for computing the orbit determination of a different Debris Object.

4.3. Numerical results

We need to know the size of the covariance matrix for the points inside the cloud and how many points we must take into the cloud. As smaller the covariance matrix is, better is the behavior of the SRIF. On the other hand, as smaller the covariance matrix is, more difficult is being right with some points close enough to the real solution (the margin of error is smaller, you must be closer to the real solution), and therefore, more points you must consider in the cloud, and more time you will require in your computations.

Table 5: Numerical simulations performed for determining the number of points inside the cloud and the initial numerical error in position and velocity.

	Points inside cloud	Position Error (km)	Position Error (km)	Percentage of SRIF divergences
Telescopes	50	0.1	0.005	8.82
	100	0.1	0.005	5.88
	500	0.1	0.005	2.94
	50	1	0.05	7.35
	100	1	0.05	1.47
	500	1	0.05	0
RADAR	50	0.001	0.005	95.24
	100	0.001	0.005	92.86
	500	0.001	0.005	73.81
	1000	0.001	0.005	73.81
	5000	0.001	0.005	57.14
	50	0.25	0.15	52.38
	100	0.25	0.15	42.86
	500	0.25	0.15	19.05
	1000	0.25	0.15	9.52
	5000	0.25	0.15	7.14
	50	2.5	1.5	19.05
	100	2.5	1.5	16.67
	500	2.5	1.5	11.90
	1000	2.5	1.5	2.38
	5000	2.5	1.5	0

In order to calibrate the good parameters of the algorithm, we have performed a set of short simulations: We have simulated different objects (GEO, MEO, GTO and OTH) (68 in case of optical measurements and 42 in case of radar). *Table 5* shows the corresponding numerical results. In the first column the number of points considered in the initial cloud is shown. The second and the third columns of *Table 5* show the value of the position and velocity sigma of the IOD error and the corresponding Covariance matrix (using the same notation as in section 4.1). The fifth column shows the percentage of objects with some SRIF divergence associated to it with respect to the simulated objects (we want this value be null).

We have considered the corresponding number of points inside the clouds and errors that for the reduced population has not diverged for analyzing the accuracy with the full population. That is σ_p =2.5km and σ_v =1. 5m/s with 500 points initially located inside the cloud (for optical measurements); and σ_p =1km and σ_v =0. 05m/s with 5000 points initially located inside the cloud (for optical measurements).

Table 6 show the numerical results for the full population. We have reduced the percentage of bad convergences from more than the 50 % up to the 2.62% in case of optical measurements and from almost 90% up to 8.6%. Moreover, we want to remark that this percentage may be decrease even more. If we consider covariance matrixes with lower sigma and more initial points (it has to be further studied the appropriate number of points), the accuracy in the orbit determination will improve.

Table 6: Accuracy of new algorithm with the full population (1448 objects for optical measurements and 1557 objects for radar measurements) during 5 simulated days.

Maximum Number of points inside cloud	Sigma in Position Error (km)	Sigma in Position Error (km)	Percentage of SRIF divergences
OPTICAL MEAUREMENTS			
500	1	0.05	2.62
RADAR MEASUREMENTS			
5000	2.5	1.5	8.6

5. CONCLUSIONS

We have developed and implemented a parallel method for orbit determination for space debris:

- It improves the results provided by classical methods (like SRIF).
  - For GB telescopes: 2.62% of divergences in front of the 48.6% obtained by applying directly SRIF.
  - For radar: 8.6% of divergences in front of the 78% obtained applying directly SRIF

The reported algorithm has been implemented in the Advanced Space Surveillance System simulator (AS4) and developed by DEIMOS Space. Moreover, the results presented in this paper are obtained during a project partially funded by the CDTI (Ministerio de Ciencia e Innovación -Spanish Government-).

6. REFERENCES

[1] E. Olmedo, N. Sánchez-Ortiz, M. R. Lerate, M. Belló-Mora, H. Klinkrad, F. Pina, "Initial Orbit Determination algorithms for cataloguing optical measurements of Space Debris", Monthly Notices of the Royal Astronomic Society, Vol. 391, pag 1259-1272, (2008)

[2] E. Olmedo, N. Sánchez-Ortiz, M. R. Lerate, M. Belló-Mora, "Design & Development of Space Surveillance System Catalogue Correlation Techniques", Final Report of ESA/ESTEC Study Contract No. 20070/06/NL/HE, 19/12/2007

[3] E. Olmedo, N. Sánchez-Ortiz, M. R. Lerate, M. Belló-Mora, H. Klinkrad, "Design and Development of correlation techniques to maintain a Space Surveillance System Catalogue", accepted at Acta Astronautica. DOI: 10.1016/j.actaastro.2009.03.024 PII: S0094576509001817

[4] Tresaco, E., Sánchez-Ortiz, N., Belló, M., Martín, J.F., Marchesi, J.E., Pina, F., "Advanced Space Surveillance System Simulator", Final Report of ESOC Contract No. 18687/04/D/HK (SC), Deimos Space S.L., 10/03/2006

[5] Bierman G.J., "Factorisation Methods for Discrete Sequential Estimation", Mathematics in Science and Engineering, Volume 128, Academic Press 1977